

Time-domain Analysis of Intermodulation Distortion of Closed-loop Class D Amplifiers

Jun Yu, Meng Tong Tan, Stephen M. Cox and Wang Ling Goh

Jun Yu and Wang Ling Goh are with the School of Electrical and Electronic Engineering, Nanyang Technological University, Singapore 639798 (e-mail: yu0002un@ntu.edu.sg; ewlgoh@ntu.edu.sg).

Meng Tong Tan is with the Agency for Science, Technology and Research (A*STAR), Institute of Microelectronics (IME), Singapore (e-mail: mengtong.tan@ieee.org).

Stephen M. Cox is with the School of Mathematical Sciences, University of Nottingham, University Park, Nottingham NG7 2RD, United Kingdom (e-mail: Stephen.cox@nottingham.ac.uk).

The manuscript has not been presented at any conferences or submitted elsewhere previously.

Abstract—This paper presents a time-domain analysis of the intermodulation distortion (IMD) of a closed-loop Class D amplifier with either 1st-order or 2nd-order loop filter. The derived expression for the IMD indicates that there exist significant 3rd-order intermodulation products (3rd-IMPs) within the output spectrum, which may lead to even greater distortion than the intrinsic harmonic components. In addition, the output expressions are compact, precise and suitable for hand calculation, so that the parametric relationships between the IMD and the magnitude and frequency of the input signals, as well as the effect of the loop filter design, are straightforwardly investigated. In order to accurately represent the IMD performance of Class D amplifiers, a modified testing setup is introduced to account for the dominantly large 3rd-IMPs when the ITU-R standard is applied.

Index Terms— Class D amplifier, Intermodulation distortion (IMD), Pulse width modulation, Time-domain modeling, 3rd-order intermodulation products

I. INTRODUCTION

Recently, there have been increasing demands on the analysis of the multi-tone response of a Class D amplifier (amp), which is quantified by the intermodulation distortion (IMD), as IMD makes music sound harsh and unpleasant [1]. Some audio engineers have even claimed that IMD is more important than harmonic distortions. Furthermore, due to the advanced fabrication technology of power MOSFETs and the enhanced linearity of the inductor and capacitor, the performance of conventional Class D amps has appreciably improved in the past decade. Thus, the intrinsic distortion caused by the feedback topology that applies to nonlinear modulation schemes becomes apparent. This work therefore aims to provide a rigorous investigation into the intrinsic IMD performance of closed-loop Class D amps.

Pulse width modulation (PWM) is still widely used in commercial Class D amps, as reported in [2-4], thanks to its simple structure, high stability, low switching frequency and effortless synchronization for multi-channel devices. Thus, PWM is broadly accepted as a benchmark to evaluate diverse modulation schemes, such as sigma-delta modulation [5], spread spectrum topology [6, 7] and self-oscillating controller [8, 9], and is the interest of this work. A typical closed-loop PWM-based Class D amp with a single feedback path is illustrated in Fig. 1. The 2nd-order loop filter provides a high loop gain inside the audio band, and hence offers great attenuation of power supply noise and power stage nonlinearity.

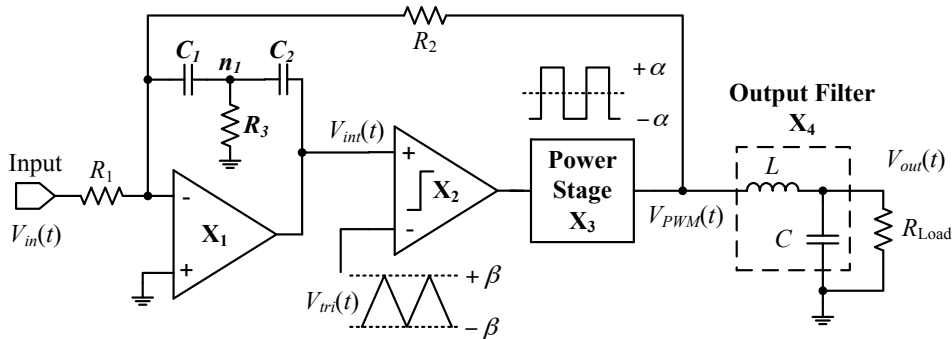


Fig. 1. Circuit schematic of a 2nd-order Class D amplifier.

We have demonstrated in [10, 11] that time-domain modeling technology, coupled with asymptotic

analysis, provides an accurate mathematical prediction of the intrinsic total harmonic distortion (THD) of PWM-based Class D amps. In this paper, we will show that this technology can also accurately predict the significant intrinsic intermodulation products in the output of closed-loop PWM-based Class D amps. Compared to previous reported work [12], our derived expressions are both much simpler and more precise; furthermore, they do not involve complicated Bessel functions, and hence enable hand calculation. Moreover, based on the characteristics of Class D amps, we propose here a modified testing setup to suitably examine the intermodulation performance of the Class D amplifier when the ITU-R standard is applied; this will be illustrated further in Section IV.

This paper is organized in the following manner. Section II briefly presents the time domain modeling of closed-loop Class D amplifiers and the analytical expression for the output signal. In Section III, IMD expressions are derived and the frequency spectrum of the output signal with two-tone stimulus is examined. The analytical results are verified in Section IV based on MATLAB and HSPICE simulations as well as hardware measurements on Printed Circuit Board (PCB). Our conclusions are drawn in Section V.

II. TIME-DOMAIN MODELING OF CLOSED-LOOP CLASS D AMPLIFIER

The intrinsic distortion of a closed-loop Class D amplifier is due to the feedback loop that is applied to the nonlinear pulse width modulator. The residual carrier ripples inside the output signal of the loop filter cause timing errors in the switching times of the modulated high frequency pulse signal (PWM signal). These timing errors are input signal dependent and hence cause intrinsic distortion in the form of both harmonic distortion and intermodulation distortion on the demodulated output signal. This phenomenon was also well explained in [13] in the frequency domain as an aliasing error. When the pulse width modulator samples the modulating signal twice per carrier period, the high frequency components surrounding multiples of carrier frequency at the output of the loop filter will be shifted back into the audio range. In a well-designed Class D amplifier, the intrinsic distortions dominate the linearity performance

when the input signal is large and at high frequency.

Due to the nonlinear nature of the closed-loop Class D amplifier, the analysis of the whole system is quite difficult and prior attempts [12, 13] had generally been more ad hoc and subjected to uncontrolled approximations. A large-signal time-domain modeling methodology was first introduced in [10] to analyze the nonlinearity of a 1st-order Class D amp. Through the rigorous derivation process, the time-domain modeling is able to accurately predict the audible frequency components in the output spectrum. A more systematic, and hence easier to understand, time-domain analysis was reported in our previous work [11] to model the output signal of a 2nd-order loop filter Class D amp; in addition, an explicit stability criterion was introduced to avoid the pulse skipping problem.

Fig. 2 depicts a generalized model of a closed-loop Class D amplifier with either 1st-order or 2nd-order loop filter. The carrier signal $v(t)$ and the PWM output signal $g(t)$ are normalized to ± 1 in order to simplify the analysis; this normalization procedure does not affect the generality of the model. The feedforward path with a constant gain equal to $-k$ can be used to reduce the distortion of the fundamental output signal. The model parameters, c_1 and c_2 , and the input signal, $s(t)$, (indicated in Fig. 2) are derived in Table I, where the passive components and the signals are referred to the circuit schematic shown in Fig. 1. Note that the two capacitors in Fig. 1, C_1 and C_2 , are assumed to be of equal values, which is a common practice in commercial design [14]. For a 1st-order loop filter design, R_3 will be removed and the serial connected C_1 and C_2 can be represented by a single capacitor C_0 with value equal to $C_1/2$.

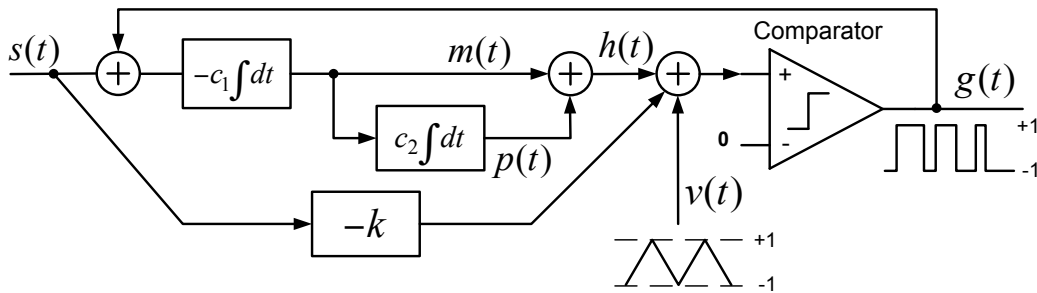


Fig. 2. General mathematical model of a closed-loop Class D amplifier.

TABLE I

MATHEMATICAL MODEL PARAMETERS

	First order loop filter	Second order loop filter
c_1	$(\alpha / \beta) \cdot (1 / R_2 C_0)$	$(\alpha / \beta) \cdot (2 / R_2 C_1)$
c_2	0	$1 / (2R_3 C_1)$
$s(t)$	$(R_2 / R_1) \cdot (v_{in}(t) / \alpha)$	

The time-domain modeling process can be divided into three steps: First, we model the switch-mode system using a set of nonlinear difference equations which relate the state of the circuit at successive switching instants. The state variables consist of the switching times of the PWM signal and integrator outputs, $m(t)$ and $p(t)$, shown in Fig. 2. Next, we derive a perturbation solution for the state variables based on a small parameter ε (i.e. $\varepsilon \equiv \omega T \ll 1$, where ω is a typical audio frequency and T is the carrier period). The accuracy of the solution is determined by the expansion order in ε , but the complexity of the solution also increases with the order of ε . Finally, we extract the audio-frequency contents, $g_a(t)$, from the PWM signal and substitute the perturbation solution of the system states into this expression. The audible output components of closed-loop Class D amps with either 1st-order or 2nd-order loop filter are expressed in (1) and (2), respectively. More details can be found in [10, 11].

Equation (2) is interpreted as follows. The first term on the right-hand side of (2) represents the desired input signal component contained in the output PWM signal, which will be referred to as the fundamental output component in the rest of the paper. The minus sign is due to the feedback topology design, which does not affect the linearity of the amplifier. The second term is proportional to the second derivative of the input signal. The third term is proportional to the second derivative of the cube of the input signal. The effect of the last two terms on the linearity of the amplifier will be examined in the next section.

Note that the input signal in (1) and (2) may be any arbitrary signal, and is not limited to a sinusoidal signal. The term $O(\varepsilon^3)$ represents the truncation error of the analytical expression. For instance, if the input signal frequency is 1 kHz and the carrier frequency is 250 kHz, then the analytical results in (1) and (2) omit terms of the order $(2\pi/250)^3$, i.e. of the order 10^{-5} .

When comparing the expressions for 1st-order and 2nd-order Class D amps, it is worthwhile to highlight that the intrinsic harmonic components and the intermodulation products of the 2nd-order Class D amplifier are exactly twice those with 1st-order loop filter. This is confirmed in Section IV. In Section III, we will only derive the output expression of 2nd-order Class D amplifier with two-tone input signal.

$$g_{a_1st}(t) = -s(t) - \frac{1}{48c_1^2} [48(1+k) - c_1^2 T^2] \frac{d^2}{dt^2} s(t) + \frac{1+k}{c_1} \cdot \frac{d}{dt} s(t) + \frac{T^2}{48} \frac{d^2}{dt^2} s^3(t) + O(\epsilon^3) \quad (1)$$

$$g_{a_2nd}(t) = -s(t) + \frac{1}{24c_1c_2} [24(1-k) + c_1c_2T^2] \frac{d^2}{dt^2} s(t) - \frac{T^2}{24} \frac{d^2}{dt^2} s^3(t) + O(\epsilon^3) \quad (2)$$

III. IMD OF THE CLOSED-LOOP CLASS D AMPLIFIER

Intermodulation distortion occurs when two or more signals with different frequencies are fed into a nonlinear amplifier. The sum and difference of the input frequencies are present at the output. In the actual measurement, with a two-tone stimulus signal (i.e. at frequencies equal to f_1 and f_2), the amplifier output signal will consist of the desired two sinusoidal waves plus an infinite number of intermodulation products (IMPs) at frequencies equal to

$$|mf_1 \mp nf_2| \quad (3)$$

where m and n are all possible integers. The “order” of any particular IMP is the sum of the absolute values of m and n . IMD is usually expressed as the ratio of RMS summation of the IMPs to the magnitude of the higher frequency component:

$$IMD_K (\%) = \frac{\sqrt{\sum_{m=1}^{K-1} \sum_{n=1}^{K-m} (V_{m \cdot f_2 - n \cdot f_1}^2 + V_{m \cdot f_2 + n \cdot f_1}^2)}}{V_{f_2}} \times 100 \quad (4)$$

where V_{f_2} is the frequency component of the output signal at frequency f_2 , and $V_{mf_2+nf_1}$ is the voltage at frequency equal to $m \cdot f_2 + n \cdot f_1$ etc. The subscript K indicates the maximum order of the IMPs that is

considered in the IMD calculation. Note that this expression is slightly different from that given in [12] for SMPTE test. In this paper, we will consistently employ the expression (4), even in the SMPTE test, to ensure that the results remain compatible with other IMD tests.

To derive the expression for IMD, we denote the angular frequencies of the two input signals by ω_1 and ω_2 , with the input signal expressed as follows:

$$s(t) = s_1 \cdot \sin(\omega_1 \cdot t) + s_2 \cdot \sin(\omega_2 \cdot t) \quad (5)$$

where s_1 and s_2 are the magnitudes of the respective input frequency components. Consequently, the expression for $g_a(t)$ is derived in (6) at the bottom of the page.

$$\begin{aligned} g_{a_2nd}(t) = & -s_1 \sin(\omega_1 t) - s_2 \sin(\omega_2 t) - \frac{3}{32} s_1^3 \omega_1^2 T^2 \sin(3\omega_1 t) - \frac{3}{32} s_2^3 \omega_2^2 T^2 \sin(3\omega_2 t) \\ & + \left(\frac{(k-1)}{c_1 c_2} - \frac{1}{24} T^2 + \frac{1}{32} T^2 s_1^2 + \frac{1}{16} T^2 s_2^2 \right) \omega_1^2 s_1 \sin(\omega_1 t) + \left(\frac{(k-1)}{c_1 c_2} - \frac{1}{24} T^2 + \frac{1}{32} T^2 s_2^2 + \frac{1}{16} T^2 s_1^2 \right) \omega_2^2 s_2 \sin(\omega_2 t) \\ & + \frac{1}{32} s_1^2 s_2 T^2 (2\omega_1 - \omega_2)^2 \sin((2\omega_1 - \omega_2)t) + \frac{1}{32} s_1 s_2^2 T^2 (2\omega_2 - \omega_1)^2 \sin((2\omega_2 - \omega_1)t) \\ & - \frac{1}{32} s_1^2 s_2 T^2 (2\omega_1 + \omega_2)^2 \sin((2\omega_1 + \omega_2)t) - \frac{1}{32} s_1 s_2^2 T^2 (\omega_1 + 2\omega_2)^2 \sin((\omega_1 + 2\omega_2)t) \end{aligned} \quad (6)$$

Equation (6) is interpreted as follows. The first two terms on the right-hand side of (6) represent the desired fundamental components. The third and fourth terms correspond to the 3rd-order harmonic distortion terms, which are the same as that derived based on a single tone input signal in [11] and not affected by the other input signal up to the leading order of analytical expression. The fifth and sixth terms signify the distortion on the magnitude of the two fundamental components; such distortion is proportional to the square of the respective input signal frequency. Compared to the output expression reported in [11], for a single-tone input signal, there exists an additional term in each fundamental distortion expression, which is proportional to the squared magnitude of the other input signal. This indicates that there exists intermodulation on the magnitude of the fundamental output components. To the best of our knowledge, this is the first reported work to quantify this phenomenon. The last four terms stand for the third order intermodulation products (3rd-IMPs). An indication of the size of the truncation error involved in (6) is

given by $(\omega_1 \cdot T)^3$ or $(\omega_2 \cdot T)^3$. The characteristics of the 3rd-IMPs are summarized as follows:

- a) The 3rd-IMPs are proportional to the magnitude of the input signal with the power equal to the absolute value of the coefficient of the input frequency forming the frequency of the 3rd-IMPs. For instance, the magnitude of the 3rd-IMP at frequency $2\omega_1 - \omega_2$ is proportional to $s_1^2 s_2$, whose power factors (i.e. 2 for s_1 and 1 for s_2) are equal to the absolute coefficients of ω_1 and ω_2 that form the frequency of the 3rd-IMP, $2\omega_1 - \omega_2$, which is again 2 for ω_1 and 1 for ω_2 .
- b) The IMPs are inversely proportional to the square of the carrier frequency, and hence increasing the carrier frequency can dramatically reduce IMD. However, the power efficiency of the amplifier will drop with the increased carrier frequency.
- c) Unfortunately, the IMPs are independent of the loop filter parameters and cannot be attenuated by adjusting the location of the zero and DC gain. As the result disagree with the conclusion of [12], an analysis on its correctness is provided below and further verification through hardware testing is given in Section IV.

Fig. 3 illustrates the MATLAB simulation results of the significant 3rd-IMPs when the loop filter parameter c_2 of a 2nd-order Class D amplifier reduces from a typical value to 0. It confirms that in a broad range, the IMPs are almost independent of the loop filter parameter. Of course, it should be borne in mind that when the zero of the 2nd-order loop filter is shifted to the origin (i.e. the limiting case of $c_2 = 0$ as indicated by the linearized loop gain transfer function, $c_1(s+c_2)/s^2$), the intrinsic intermodulation distortion should converge with that of the 1st-order Class D amplifier and be reduced by half. This is demonstrated in Fig. 3 and it means that the IMD is not completely independent of the loop filter design. Unfortunately, it is not possible to predict the convergence from a 2nd-order Class D amplifier to a 1st-order Class D amplifier using the expressions in this paper. This is because the derivation of (2) relies on fixed nonzero c_1 and c_2 values, which is clear from the presence of both these parameters in the denominator of the second term in (2). Put more abstractly, Equation (6) provides an excellent approximation for “genuinely second order amplifiers” (i.e. $c_1 T = O(1)$ and $c_2 T = O(1)$), but gives a much poorer approximation for amplifiers that are

“nearly first order”.

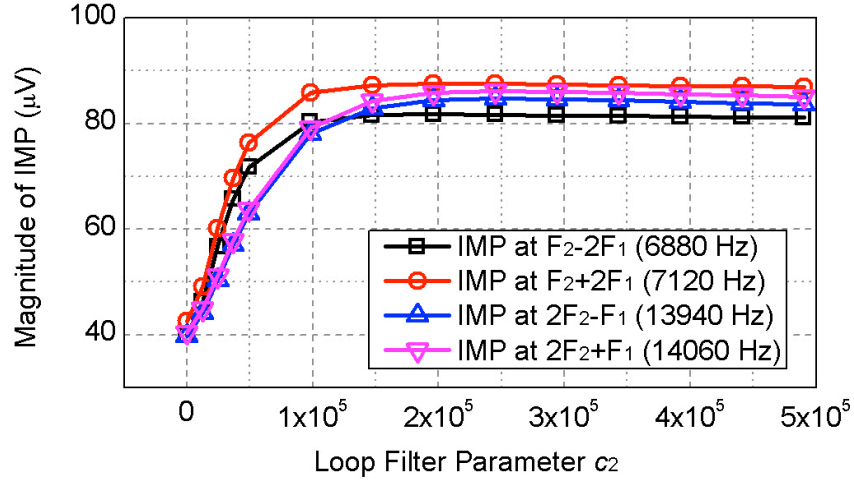


Fig. 3. Intermodulation products of a 2nd-order Class D amplifier versus the loop filter parameter c_2 . The input signal is set with

$$f_1 = 60 \text{ Hz}, f_2 = 7 \text{ kHz}, M_1 = 0.7 \text{ and } M_2 = 0.175.$$

From circuit analysis, there are two contrary effects when we adjust the loop filter parameters. On one hand, when we increase c_1 or c_2 to enhance the linearized loop gain, the low-frequency audible error between the input signal and output PWM signal is further suppressed, just like any linear system. On the other hand, the increase of c_1 and c_2 creates larger phase and duty cycle errors in the PWM signal during the modulation process through altering the waveform of the high frequency ripple signal at the output of the loop filter. The second effect is the root of the difference when applying negative feedback to a switch-mode system as compared to a linear system. As demonstrated in [13] when deriving the total harmonic distortion of a closed-loop Class D amplifier, the duty cycle error is proportional to the real part and the phase error is proportional to the imaginary part of the loop filter transfer function. The counterbalance of these two effects in a typical 2nd-order Class D amplifier causes IMD to be almost independent of the loop filter design.

Since the expression for the output signal is derived based on an ideal model of the 2nd-order Class D amp, the derived intermodulation products are produced intrinsically due to the negative feedback applied to the nonlinear pulse width modulator. Finally, the IMD expression of the 2nd-order Class D amp is derived in (7). Equation (7) indicates that IMD of the 2nd-order Class D amp is independent of the design of

the loop filter. Instead, it is determined by the frequency and amplitude of the input signals, and also the carrier frequency. Note that the slight distortion on the fundamental component is ignored to simplify the expression without notably affecting the precision.

$$IMD_3(\%) \approx \frac{1}{32} s_1 T^2 \sqrt{s_1^2 (32\omega_1^4 + 48\omega_1^2\omega_2^2 + 2\omega_2^4) + s_2^2 (32\omega_2^4 + 48\omega_1^2\omega_2^2 + 2\omega_1^4)} \times 100 \quad (7)$$

Fig. 4 shows the output spectrum of a 2nd-order Class D amplifier with a two-tone stimulus signal of 5 kHz and 6 kHz. The amplitudes of the two sinusoidal input signals are both equal to 0.3. The first pair of 3rd-IMPs are located to either side of the fundamental components (i.e. at frequencies equal to $2f_1 - f_2$ and $2f_2 - f_1$) and the other pair of 3rd-IMPs are located between the two 3rd-order harmonics (i.e. at frequencies equal to $2f_1 + f_2$ and $2f_2 + f_1$). Note that the latter two 3rd-IMPs are even larger than the 3rd-order harmonics of the input signals. This demonstrates that the IMD may have a worse effect on the linearity of a closed-loop PWM-based Class D amp than the harmonic distortion.

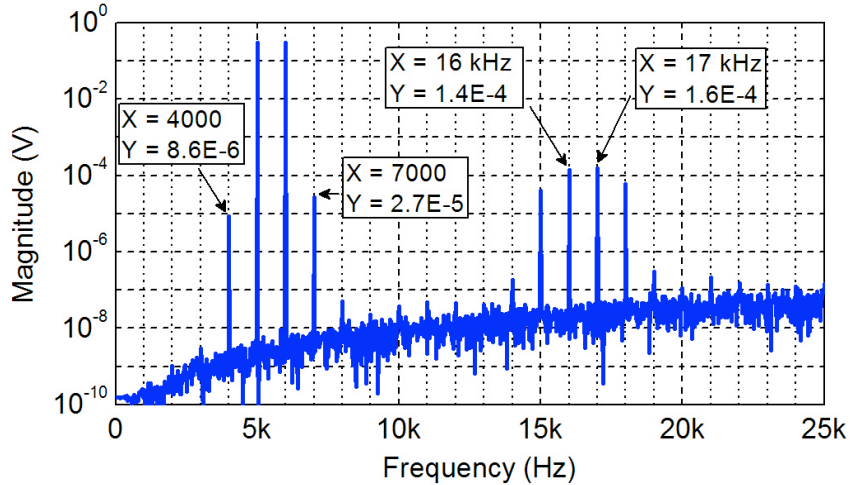


Fig. 4. Output spectrum of a 2nd-order Class D amp with two 0.3 V sinusoidal input signals that are of $f_1 = 5$ kHz and $f_2 = 6$ kHz, respectively.

The accuracy of the mathematical expression is verified by comparing the analytical results and the MATLAB simulation results as shown in Fig. 5. The results are in good agreement with each other across the modulation index range. The input signals are set with $f_1 = 60$ Hz, $f_2 = 7$ kHz and $M_2 = M_1/4$, which are a typical SMPTE testing setup that will be further explained in Section IV. As illustrated in Fig. 5, the

analytical results precisely predict the magnitudes of all the significant frequency components - the two fundamental components in Fig. 5(a) and Fig. 5(b) and the four 3rd-IMPs (see Fig. 5(c)-(f)) with varying M_2 setting (ranging from 0.025 to 0.175).

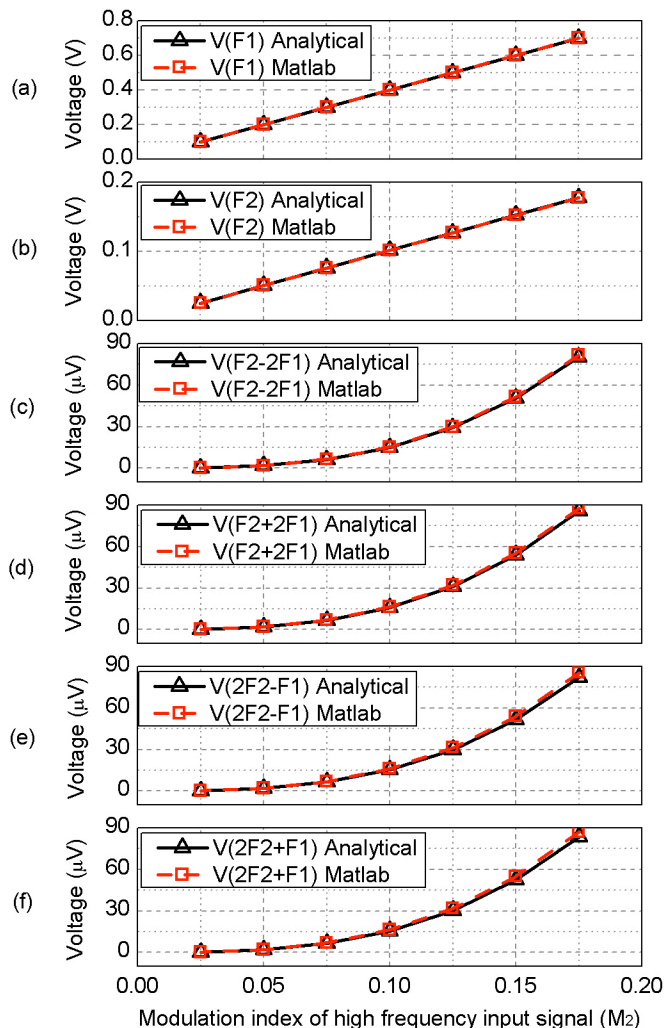


Fig. 5. Matching between analytical and MATLAB simulation results for all significant frequency components in a typical SMPTE test: (a)-(b) the two fundamental frequency components; (c)-(f) the four 3rd-IMPs.

IV. ANALYTICAL, SIMULATION AND MEASUREMENT RESULTS

In this section, the analytical derivations of IMD are verified by comparing the derived expressions against MATLAB simulation, HSPICE simulation, and also experimental measurements on a Class D amp

built on PCB using discrete components as shown in Fig. 6. Both 1st-order and 2nd-order loop filter designs are tested using this board by inserting or removing the resistor, R_3 , shown in Fig. 1.

Furthermore, in order to verify the effect of the loop gain parameters on the intrinsic IMD, two different 2nd-order loop filters (Design I and II) have been tested. The loop filter design parameters are tabulated in Table II and the respective linearized loop gains are plotted in Fig. 7. Note that the feedforward gain k in Fig. 2 is equal to 0 for all the loop filters used here. The output low pass filter is designed as $L = 33 \mu\text{H}$, $C = 0.242 \mu\text{F}$ and $R_L = 8 \Omega$. In the absence of specification to the contrary, the carrier switching frequency is set to 250 kHz by default. Note that the 2nd-order loop filter with Design II parameters achieved a 6 dB higher low-frequency gain as compared to that with the Design I parameters recommended in [2].

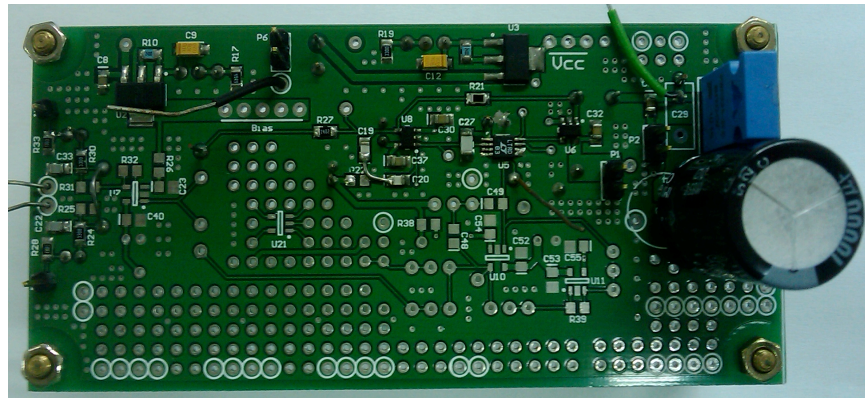


Fig. 6. Hardware implementation for IMD testing.

TABLE II

MODEL PARAMETERS OF DIFFERENT LOOP FILTER DESIGNS

Parameter	2 nd -order Design I [2]	2 nd -order Design II	1 st -order Design
c_1	4.3301e5	4.988e5	4.988e5
c_2	2.8868e5	4.9034e5	0

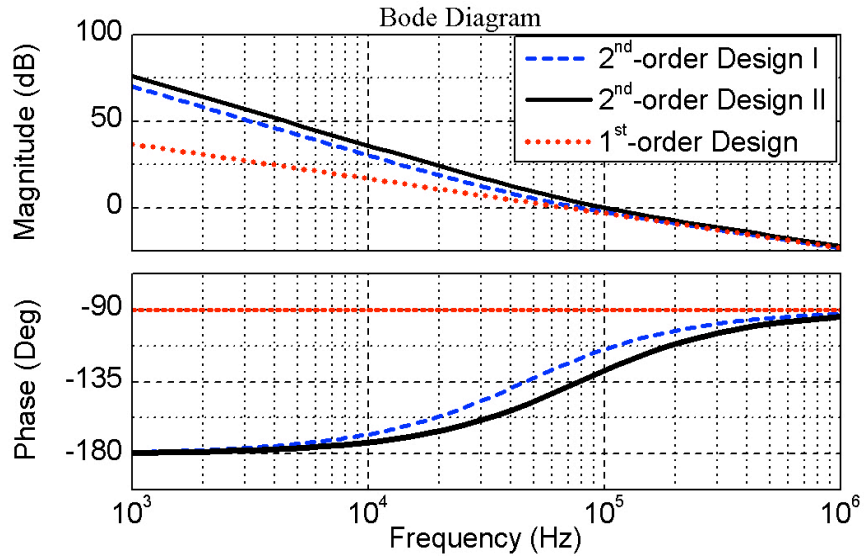


Fig. 7. Plots of linearized loop gains of the closed-loop Class D amps based on different loop filter designs provided in Table II.

The most common IMD measurement standard in the professional, broadcast, and consumer audio fields is set by the Society of Motion Picture and Television Engineers (SMPTE) and is referred as SMPTE method, in which a two-tone test signal consisting of a low-frequency high-amplitude tone (60 Hz) is linearly combined with a high-frequency tone (7 kHz) at 1/4 the amplitude (-12 dB) of the low-frequency tone [15].

Fig. 8 depicts the frequency spectrum of the output signal in a typical SMPTE IMD test in MATLAB simulation. In this case, the intermodulation products are located at the sidebands of the high-frequency tone and its harmonics (i.e. 3rd-IMPs at $f_2 \pm 2f_1$ and $2f_2 \pm f_1$). Note that although the spectrum lacks any 2nd-order harmonic component (i.e. at 14 kHz), IMPs around the second harmonic do exist. In addition, Fig. 8 also demonstrates that there are no 2nd-IMPs, and hence corroborates the prediction based on (6).

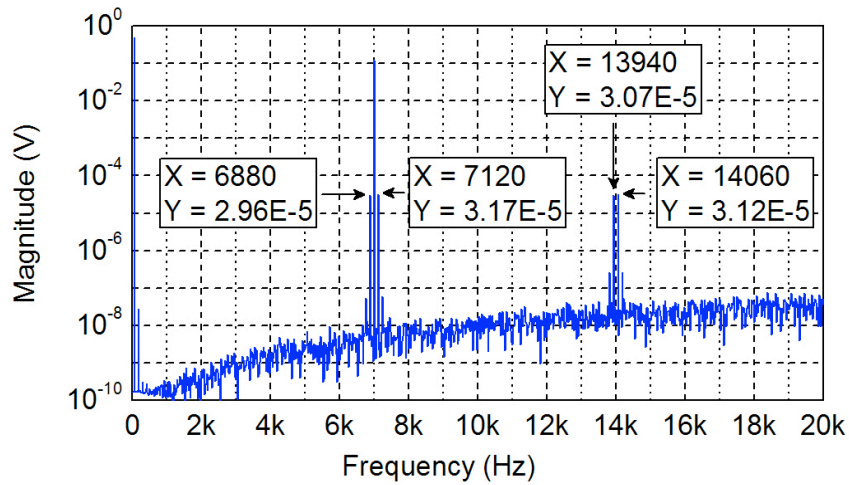


Fig. 8. Output spectrum of a 2nd-order Class D amp with two sinusoidal input signals of 60 Hz and 7 kHz, with amplitudes of 0.5 V and 0.125 V, respectively.

Fig. 9 depicts the SMPTE IMD of the 2nd-order Class D amp against the modulation index of the high-frequency input component. To ensure that the combined input magnitude is less than 1, the modulation index of the 60 Hz input signal varies from 0.1 to 0.7 and the modulation index of the 7 kHz input signal varies from 0.025 to 0.175 respectively. The loop filter deployed in the amplifier is designed using the Design I parameters stated in Table II.

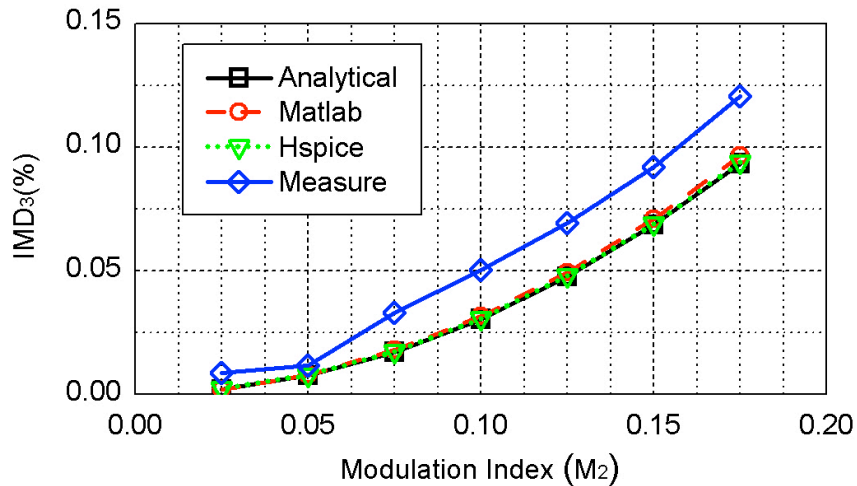


Fig. 9. SMPTE IMD of the 2nd-order Class D amp versus the modulation index of the 7 kHz input signal with loop filter Design

I.

As evident in Fig. 9, the analytical results agree well with the two simulation outcomes, i.e. MATLAB

and HSPICE. Furthermore, the IMD is proportional to the square of the modulation index of the high frequency input tone. This can be explained using (7) by substituting s_1 with $4 \cdot s_2$. The measurement results have the same increasing trend as the analytical results. The mismatch between the simulation and the measurement results is probably due to the non-ideality of the power MOSFETs and the nonlinearity of the decoupling LC filter. This was investigated through an experiment in which the LC filter and the 8Ω load are replaced by a 3rd-order RC filter with an almost identical cut-off frequency. As the RC filter draws much less current than the LC filter with a resistive load, the effect of the on-resistance can be ignored and the PWM waveform at the output of the power stage achieves sharper rising and falling edges. It is interesting to note that by replacing the LC filter with the RC filter, the non-ideality of the power stage is also minimized. The measured IMD under such condition is much closer to the analytical result as compared to that with the LC filter. Through this experiment, it is reasonable to conclude that the discrepancy between the measurement results and the analytical results is mainly due to the non-idealities of the power stage and the output filter. A comprehensive analysis on the non-ideality of the power stage was reported in [16]. Fig. 9 also reveals that by appropriately choosing the inductor and capacitor, and also using well-designed power MOSFETs, the intermodulation distortion of a 2nd-order Class D amp is dominated by the intrinsic IMD, especially when the input signal is large.

After modifying the 2nd-order loop filter based on the Design II parameters provided in Table II, a 6 dB higher loop gain is achieved. The IMD versus modulation index of the high-frequency tone is re-plotted in Fig. 10 using this modified loop filter. The simulation results match the analytical results and remain unchanged as compared to that seen in Fig. 9. Hence, we have verified that the intrinsic IMD is independent of the loop filter design. This is a very important characteristic of both the intrinsic harmonic distortion and intermodulation distortion. Furthermore, we note that the measured IMD in Fig. 10 is smaller than that of Fig. 9. This is due to the additional suppression on the non-ideality effect of the power stage, due to the increased linearized loop gain.

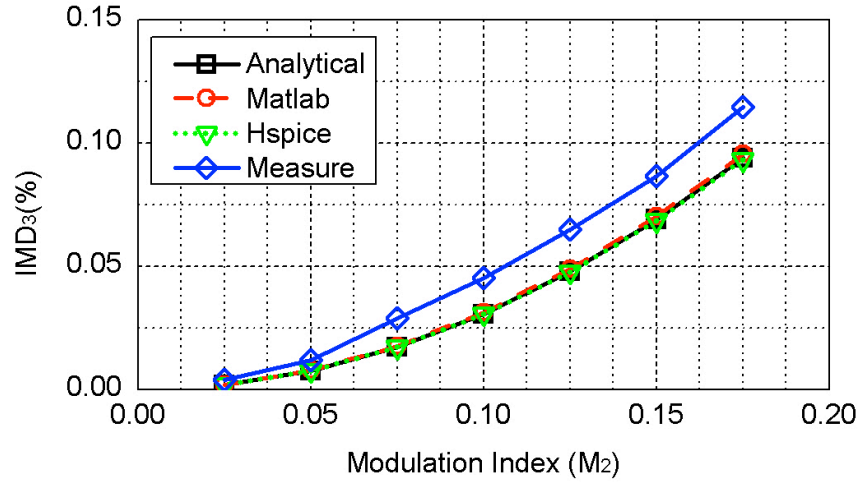


Fig. 10. SMPTE IMD of the 2nd-order Class D amp versus the modulation index of the 7 kHz input signal with loop filter Design

II.

Fig. 11 illustrates the IMD performance of a 1st-order Class D amp. The 1st-order loop filter is achieved by removing the resistor R_3 from the 2nd-order loop filter with Design II parameters. Comparing with the results of the 2nd-order Class D amp shown in Fig. 10, the simulated IMD of the 1st-order Class D amp is reduced by half and matches well with the analytical results. However, there exists significant mismatch between the measurement results and the simulation results. This is mainly due to the much lower loop gain of the 1st-order Class D amp where it is unable to sufficiently attenuate the distortions introduced by the practical power stage. This is also reflected in the HSPICE simulation results when the input signal is small. As the intrinsic distortion reduces quadratically with the decreasing magnitude of the input signal, the power stage distortion becomes the dominant factor that determines the linearity of the Class D amplifier and cannot be predicted by (6). Consequently, the deviation between the analytical results and HSPICE simulation results becomes larger at small modulation index.

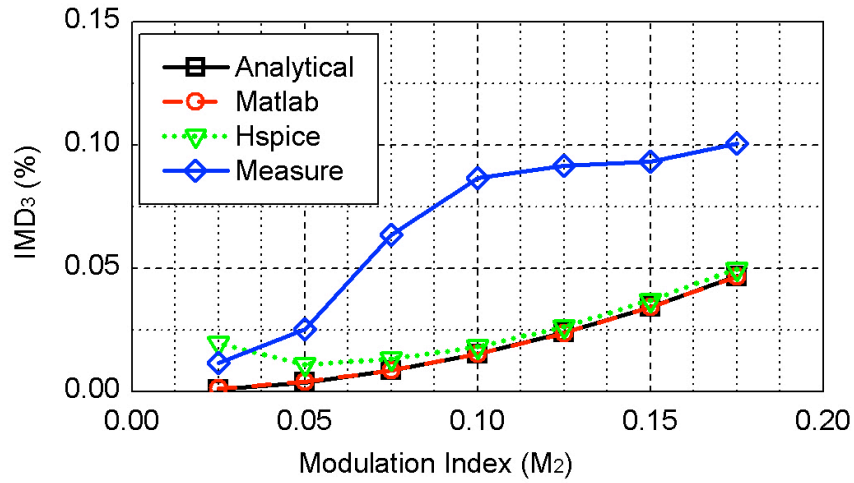


Fig. 11. SMPTE IMD of a 1st-order Class D amp versus the modulation index of the 7 kHz input signal.

As a short summary, although a 1st-order Class D amp can achieve a lower intrinsic IMD, its overall performance may be worse than that of a 2nd-order Class D amp. Hence, to achieve a good overall performance, a 2nd-order loop filter is always preferred and the gain of the loop filter inside the audio band should be as high as possible. Furthermore, in order to improve the linearity of a closed-loop pulse width modulated Class D amplifier, more research on circuit structure should be established; some relevant work has been reported in [10, 17]. In the rest of this section, all the verification is based on the 2nd-order loop filter with Design II parameters, which manages to achieve a maximized attenuation of the non-ideality of the power stage and supply noise, hence yielding more accurate results on the intrinsic IMD of the closed-loop Class D amp.

Fig. 12 depicts the IMD performance of a 2nd-order Class D amplifier versus the frequency of the low-frequency tone inside the two-tone input signal, i.e. from 60 Hz to 6 kHz, while fixing the high-frequency tone at 7 kHz. This test is used to examine the relationship between the magnitude of the IMPs and the frequencies of the input signal. As illustrated in Fig. 12, the analytical results are noted to match well with the simulation and measurement results. It is also worthwhile to highlight that when the low-frequency input signal shifts towards the high-frequency tone, the intermodulation distortion increases significantly.

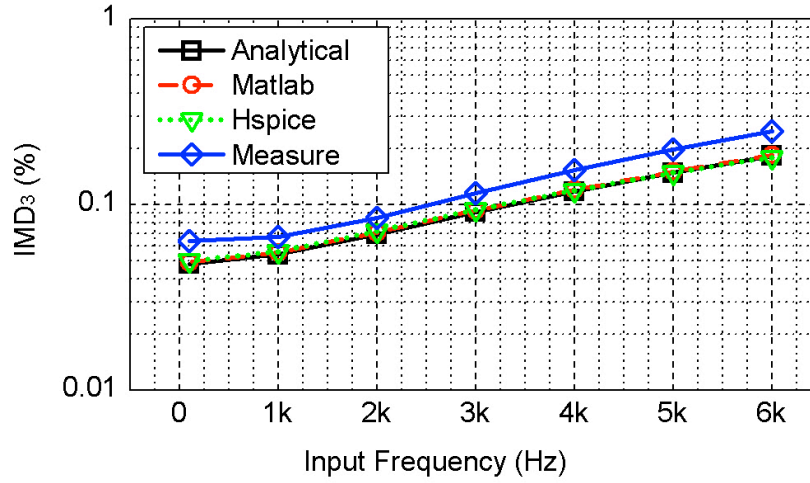


Fig. 12. SMPTE IMD versus f_1 for 2nd-order Class D amplifier with Design II parameters at $M_1 = 0.5$, $M_2 = 0.125$ and $f_2 = 7$ kHz.

Fig. 13 demonstrates the relationship between the carrier switching frequency of the Class D amp and the IMD. The input signal has the following settings: $f_1 = 60$ Hz, $f_2 = 7$ kHz, $M_1 = 0.7$, $M_2 = 0.175$. Note that the IMD decreases dramatically with increasing switching frequency, similar to the THD, and the analytical results accurately predict the trend of the rapid diminishing of the intermodulation distortion. As the loop filter Design II parameters used in the test were optimized based on a typical carrier frequency of 250 kHz, when the carrier frequency is reduced to 200 kHz, the output of the pulse width modulator may fail to switch inside a carrier period. This phenomenon has been explained in [11] as "pulse skipping", which is similar to the "fast-scale" instability issue described in [18, 19] for DC-DC converters. The criterion for preventing the occurrence of the pulse skipping has been derived in [11] and is reproduced here as $c_1 c_2 T^2 < 4$. The occurrence of pulse skipping will raise the noise floor of the output signal and cause extra distortions that cannot be predicted based on (6) (shown as mismatch between the analytical result and simulation results at 200 kHz). However, since a properly designed Class D amplifier will not have pulse skipping issue, the small mismatch noted here is not a concern.

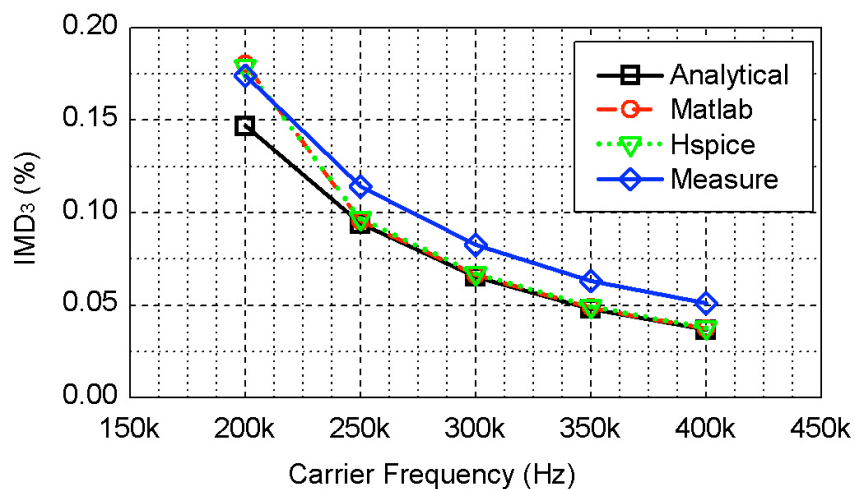


Fig. 13. IMD versus switching frequency of a 2nd-order Class D amplifier.

Another testing standard known as the “ITU-R” or “CCIF” method is also widely used by some manufacturers. This method was originally recommended by the Consultative Committee for International Telephone (CCIF), which later became the Radio communications sector of the International Telecommunications Union (ITU). The stimulus signal for this intermodulation distortion test consists of two equal-amplitude high frequency signals that are spaced rather close together in frequency. Common signal frequencies are: 13 kHz and 14 kHz for 15 kHz band-limited systems, and 19 kHz and 20 kHz for systems with a full audio bandwidth. For the often seen case of the 19 kHz and 20 kHz test, only the 1 kHz component is measured, which is the 2nd-IMP at frequency equal to $f_2 - f_1$.

Fig. 14 illustrates the output spectrum of a 2nd-order Class D amp in the ITU-R test based on MATLAB simulation. The Class D amplifier achieves an excellent IMD performance in the ITU-R test when only the 1 kHz IMP is counted. This is because the second order intermodulation products of a Class D amp are usually negligible. However, this does not mean that Class D amplifiers have good rejection on intermodulation distortion. As seen in Fig. 14, the most significant IMP within the audio band is at 18 kHz (i.e. the 3rd-IMP at $2 \cdot f_1 - f_2$). Hence, we conclude that the traditional ITU-R test is not suitable for evaluating the performance of Class D amplifiers.

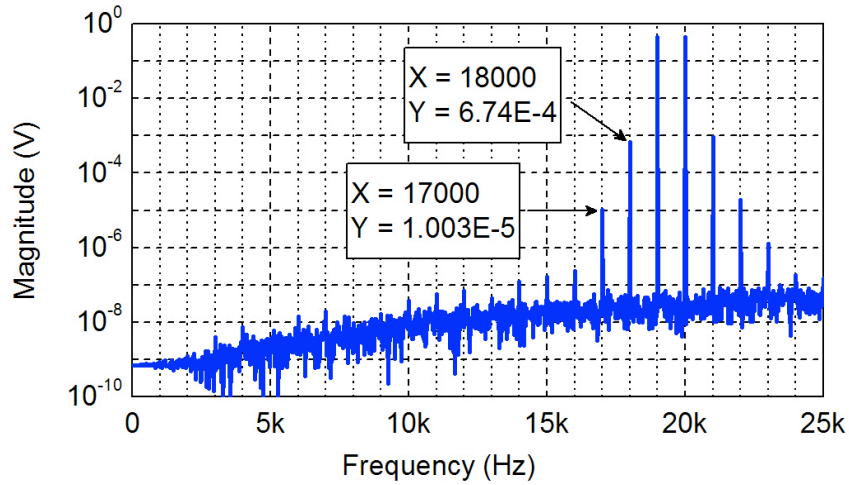


Fig. 14. ITU-R IMD MATLAB simulation result for $f_1 = 19$ kHz, $f_2 = 20$ kHz, $M_1 = M_2 = 0.45$ based on Design II parameters.

In this paper, we propose a modified testing setup that uses two input signals at the middle-band of the audio range, such as 5 kHz and 6 kHz signals, with equal modulation index. The output spectrum is as previously depicted in Fig. 4, which shows that the main 3rd-IMPs are located alongside the fundamental components and in between the two 3rd-order harmonics. Fig. 15 demonstrates the IMD performance of a 2nd-order Class D amplifier with input signals set at 5 kHz and 6 kHz, each with equal modulation index that sweeps from 0.1 to 0.45. This test clearly reflects the rapid increase of the IMD with respect to the magnitudes of the input signals.

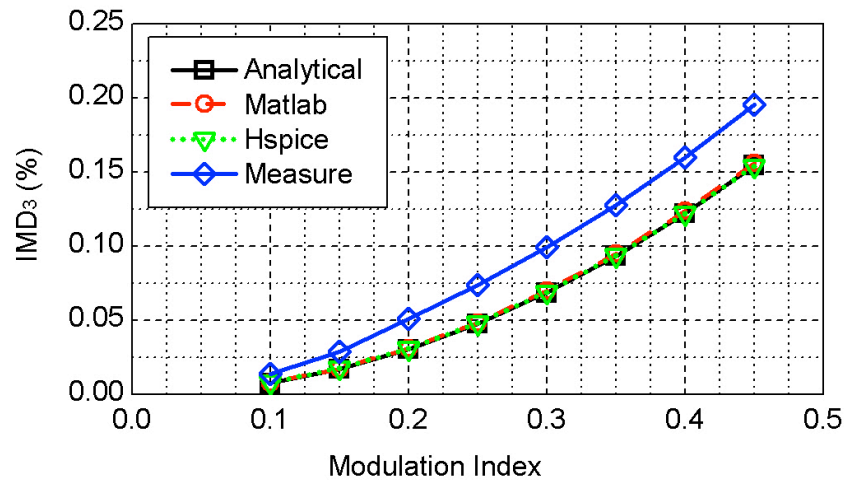


Fig. 15. IMD versus modulation index for modified ITU-R test with $f_1 = 5$ kHz, $f_2 = 6$ kHz, $M_1 = M_2$ and Design II parameters.

V. CONCLUSION

By means of large-signal time domain analysis, the intrinsic IMD expressions for closed-loop PWM-based Class D amps with either 1st-order or 2nd-order loop filter were investigated. The derived expressions are simple, accurate and clearly reflect the relationship between the input signal, carrier frequency and the IMPs. The results obtained demonstrate that although negative feedback can reduce the distortion due to the non-ideality of the power stage, it can cause significant undesired IMD, even larger than the intrinsic harmonic distortion. Furthermore, the results demonstrated that a Class D amp with 1st-order loop filter has an intrinsic IMD half that of the 2nd-order loop filter. Nevertheless, for a broad range of parameters, the IMD is independent of the parameters of a fixed loop filter structure. In addition, Class D amplifiers contain only odd order intrinsic intermodulation products and hence the traditional ITU-R test is not suitable for Class D amplifiers. To correctly characterize the intermodulation distortion performance of a Class D amplifier, a modified test setting is suggested when the ITU-R standard is applied.

REFERENCES

- [1] D. Bohn, "Audio Specifications," Rane Corporation, 2000.
- [2] M. Berkhout, "An integrated 200-W class-D audio amplifier," *IEEE J. Solid-State Circuits*, vol. 38, pp. 1198-1206, 2003.
- [3] I. Deslauriers, N. Avdiu, and O. Boon Teck, "Naturally sampled triangle carrier PWM bandwidth limit and output spectrum," *IEEE Trans. Power Electron.*, vol. 20, pp. 100-106, 2005.
- [4] C. Pascual, *et al.*, "High-fidelity PWM inverter for digital audio amplification: Spectral analysis, real-time DSP implementation, and results," *IEEE Trans. Power Electron.*, vol. 18, pp. 473-485, 2003.
- [5] E. Gaalaas, B. Y. Liu, N. Nishimura, R. Adams, and K. Sweetland, "Integrated Stereo $\Delta\Sigma$ Class D Amplifier," *IEEE J. Solid-State Circuits*, vol. 40, pp. 2388-2397, 2005.
- [6] M. Xin, C. Zao, Z. Ze-kun, and Z. Bo, "An Advanced Spread Spectrum Architecture Using Pseudorandom Modulation to Improve EMI in Class D Amplifier," *IEEE Trans. Power Electron.*, vol. 26, pp. 638-646, 2011.
- [7] M. L. Yeh, W. R. Liou, H. P. Hsieh, and Y. J. Lin, "An Electromagnetic Interference (EMI) Reduced High-Efficiency Switching Power Amplifier," *IEEE Trans. Power Electron.*, vol. 25, pp. 710-718, 2010.
- [8] M. C. W. Høyerby and M. A. E. Andersen, "Carrier Distortion in Hysteretic Self-Oscillating Class-D Audio Power Amplifiers: Analysis and Optimization," *IEEE Trans. Power Electron.*, vol. 24, pp. 714-729, 2009.
- [9] G. Pillonnet, R. Cellier, E. Allier, N. Abouchi, and A. Nagari, "A topological comparison of PWM and hysteresis controls in switching audio amplifiers," in *Proc. APCCAS*, 2008, pp. 668-671.
- [10] S. M. Cox and B. H. Candy, "Class-D audio amplifiers with negative feedback," *SIAM J. Appl. Math.*, vol. 66, pp. 468-488, 2006.

- [11] S. M. Cox, M. T. Tan, and J. Yu, "A second-order Class-D audio amplifier," *SIAM J. Appl. Math.*, vol. 71, pp. 270-287, 2011.
- [12] W. Shu and J. S. Chang, "IMD of Closed-Loop Filterless Class D Amplifiers," *IEEE Trans. Circuits and Systems I: Reg. Papers*, vol. 57, pp. 518-527, 2010.
- [13] L. Risbo and C. Neesgaard, "PWM Amplifier Control Loops with Minimum Aliasing Distortion," in *AES 120th Convention*, Paris, France, 2006.
- [14] "TDA7490 25W+25W stereo Class-D amplifier 50W MONO in BTL," ST semiconductor.
- [15] B. Metzler, *Audio Measurement Handbook*: Audio Precision Inc., 1993.
- [16] L. Risbo and M. C. W. Hoyerby, "Suppression of continuous-time and discrete-time errors in switch-mode control loops," in *AES 37th International Conference*, Hillerod, Denmark, 2009.
- [17] B. H. Candy and S. M. Cox, "Improved analogue class-D amplifier with carrier symmetry modulation," in *AES 117th Convention*, San Francisco, CA, USA, 2004.
- [18] S. K. Mazumder, A. H. Nayfeh, and D. Boroyevich, "Theoretical and experimental investigation of the fast- and slow-scale instabilities of a DC-DC converter," *IEEE Trans. Power Electron.*, vol. 16, pp. 201-216, 2001.
- [19] S. K. Mazumder, A. H. Nayfeh, and D. Boroyevich, "An investigation into the fast- and slow-scale instabilities of a single phase bidirectional boost converter," *IEEE Trans. Power Electron.*, vol. 18, pp. 1063-1069, 2003.